fluids

MDPI

Article

Rheological and Microstructural Properties of Oil-in-Water Emulsion Gels Containing Natural Plant Extracts Stabilized with Carboxymethyl Cellulose/Mango (*Mangifera indica*) Starch

Luis Mieles-Gómez [1], Santander E. Lastra-Ripoll [1], Edilbert Torregroza-Fuentes [2], Somaris E. Quintana [1] and Luis A. García-Zapateiro [1,*]

[1] Research Group of Complex Fluid Engineering and Food Rheology, University of Cartagena, Cartagena 130015, Colombia; lmielesg@unicartagena.edu.co (L.M.-G.); slastrar@unicartagena.edu.co (S.E.L.-R.); squintanam@unicartagena.edu.co (S.E.Q.)

[2] Research Group Science Technology and Society—CTS, University of Cartagena, Cartagena 130015, Colombia; etorregrozaf@unicartagena.edu.co

* Correspondence: lgarciaz@unicartagena.edu.co; Tel.:+57-5-675-20-24 (ext. 205)

Abstract: Emulsion gels are an alternative to developing food products and adding bioactive compounds; however, different stabilizers have been employed considering natural ingredients. In this work, stabilization of emulsion gels with blends of carboxymethylcellulose and kernel mango starch was performed with the addition of mango peel extracts, evaluating their physical, rheological and microstructural properties. Phenolic extract from mango peels (yields = 11.35 ± 2.05% *w/w*), with 294.60 ± 0.03 mg GAE/100 g of extract and 436.77 ± 5.30 µMol Trolox/g of the extract, was obtained by ultrasound-assisted extraction (1:10 peel: Ethanol *w/v*, 200 W, 30 min), containing pyrogallol, melezitose, succinic acid, γ-tocopherol, campesterol, stigmasterol, lupeol, vitamin A and vitamin E. In addition, mango kernel starch (yields = 59.51 ± 1.35% *w/w*) with 27.28 ± 0.05% of amylose was obtained, being the by-product of mango (*Mangifera indica* var fachir) an alternative to producing natural food ingredients. After that, stable emulsions gels were prepared to stabilize with carboxy methylcellulose–kernel mango starch blends and mango peel extracts. These results provide an ingredient as an alternative to the development of gelled systems. They offer an alternative to elaborating a new multifunctional food system with bioactive properties with potential application as a fat replacement or delivery system in the food industry.

Keywords: oil-in-water emulsion gel; carboxymethyl cellulose; mango starch; mango peel extracts; rheological properties

Citation: Mieles-Gómez, L.; Lastra-Ripoll, S.E.; Torregroza-Fuentes, E.; Quintana, S.E.; García-Zapateiro, L.A. Rheological and Microstructural Properties of Oil-in-Water Emulsion Gels Containing Natural Plant Extracts Stabilized with Carboxymethyl Cellulose/Mango (*Mangifera indica*) Starch. *Fluids* **2021**, *6*, 312. https://doi.org/10.3390/fluids6090312

Academic Editor: Mehrdad Massoudi

Received: 27 July 2021
Accepted: 27 August 2021
Published: 1 September 2021

1. Introduction

Emulsion gels or gelled emulsions (EGs) are defined as emulsions with a gel-like network structure and mechanical properties [1,2] with potential used for the development of meat products [3] and, in the emulsified system, with bioactive compounds [4]. EGs present interesting properties, such as the ability to solubilize and stabilize hydrophilic and hydrophobic components and provide greater thermodynamic stability during storage due to decreased movement of oil droplets and oxygen diffusion within the systems [5,6].

The development of food products with bioactive compounds represents an opportunity to improve the shelf life and health condition of the products [7,8]. Mango, and mainly its peel, is a rich source of phenolic compounds, such as gallotanins, gallic acid and mangiferin [9,10]; these compounds have been associated with solid antioxidant effects and benefits for therapeutic properties [11]. However, they could not be added directly due to inactivation or degradation under processing conditions that cause unpleasant color, bitterness, or astringency, indicating that protecting phenols using emulsion procedures could overcome such drawbacks [12]; EG is an alternative to the incorporation of phenolic compounds in food products.

The development of convectional EG essentially involves the production of an emulsion using high amounts of emulsifying agents (5–50%) [13] and gelling agents, such as hydrocolloids in the continuous phase [14–16]. For emulsion products, polysaccharides, such as guar gum, xanthan gum and starch, as well as carboxymethylcellulose (CMC), are the most used; this ingredient has been used in mixtures for the stabilization of emulsions due to the synergistic interaction among other components, which contribute to desirable rheological properties [17]; also, it overcomes the specific weakness of individual polysaccharides in terms of their functionality [18].

Carboxymethylcellulose (CMC), a water-soluble cellulose derivative, is an anionic polysaccharide employee that provides good uniformity of droplet size in oil–water emulsion [19], due to the high water-binding capacity of the carboxymethyl functional groups, which prevent phase separation [19]. However, in highly concentrated emulsion products, the use of CMC is not practiced, due to the lack of its ability to give a gel-like structure with a low yield stress value [20].

Starch granules are becoming a good particle stabilizer for EG, due to their ability to emulsify, to form gel and their contribution to a wide variety of food products [21,22]. Mango kernel starch is a low-cost non-conventional starch generated from mango processing waste and has had a wide variety of applications in food matrices, such as encapsulation, edible coating, or as a food additive. Therefore, more studies are needed to overcome the current problem concerning the use of polysaccharides in addition to a binary mixture of polysaccharides by introducing ternary mixtures of polysaccharides into emulsion products. This study focused on stabilizing EG with blends of CMC and kernel mango starch with mango peel extracts and evaluated their chemical, rheological and microstructural properties.

2. Materials and Methods

2.1. Chemical Preparation

Ethanol (99.5% purity) was purchased from Panreac (Barcelona, Spain), anhydrous sodium carbonate (99.5% purity), gallic acid standard (>98% purity), phenyl methyl siloxane (5%), Folin–Ciocalteu reagent, tween-80, 2,2′-azino-bis (3-ethylbenzothiazoline-6-sulfonic acid) diammonium salt (ABTS, ≥95% purity) and potato amylose from Sigma-Aldrich (St. Louis, MO, USA) and CMC from Tecnas S.A. (Medellín, Colombia).

2.2. Sample Preparation

Mango (*Mangifera indica* var fachir) cultivated in the Department of Bolívar (Colombia) were provided in commercial maturity. Washing was performed to clean the fruit using warm tap water and sodium hypochlorite (100 ppm); then, the peel, seed and pulp were manually separated.

The seeds were washed to remove any adhering pulp traces, then dried at 40 °C for 4 h in a hot air tray dryer to facilitate the separation of the kernel and the hull; then, the kernel was separated from the hull, cut and dried in a hot air tray dryer at 40 °C for 12 h and grounded (cutting–grinding head IKA MF 10.1 Germany) to obtain the flour (particle size <200 µm).

The peel was lyophilized using a Labconco Freezone 1.5 L bench top freeze dry equipment to preserve the phenolic content and ground in an IKA MF 10.2 (Germany) mill coupled with a sieve to obtain a powder with a particle size of less than 250 µm.

2.3. Ultrasound-Assisted Extraction of Mango Peel

Ultrasound-assisted extraction (UAE) was carried out following the procedure described by Lastra-Ripoll et al. [23] and Quintana et al. [7], using an ultrasonic bath with an operating frequency of 25 kHz and an input power of 200 W. The extractions were carried out for 30 min with a plant/ethanol ratio of 1:10 *w/v*, at 25 °C. The mixture was separated by filtration and dryed by rotary evaporation (IKA RV 8-V) to obtain mango peel extracts.

2.3.1. Determination of Total Phenolic Compounds (TPC) and Antioxidant Activity

The TPC content (expressed as GAE: mg of gallic acid equivalents/g of extract) was determined using the Folin–Ciocalteu method [24]. The antioxidant activity was measured employing the ABTS assay following the method described by Re et al. [25]; the results were expressed as Trolox equivalents (TEAC) (µmol Trolox/g of extract), which were calculated considering the Trolox standard and sample concentrations that produce the scavenging of 50% of $ABTS^{+}$ radical.

2.3.2. GC-MS Analysis

Identification and quantification of the bioactive compounds of mango peel extracts were carried out by GS-MS-FID using 7890D Agilent Technologies (Santa Clara, CA. USA). A DB-5 ms (Agilent, Tokyo, Japan) capillary column (30 m × 0.25 mm × 0.25 µm) was used. Chromatographic methods started at 250 °C, then increased from 120 °C to 220 °C (40 °C/min, hold time 0.5 min) and increased to 290 °C (4 °C/min, hold time 8 min). The flame induction detector temperature was 300 °C; hydrogen flow rate, 40 mL/min; air flow rate, 450 mL/min; tail gas flow rate, 1.03 mL/min; injection volume, 1.0 µL. Compounds were identified with the NIST 2014 mass spectral library. The relative content of each component was obtained using the peak area normalization method for quantification.

2.4. Extraction of Mango Kernel Starch

Mango kernel starch was isolated using a method described by Kaur [26] with some modifications. The flour was suspended in a 1% sodium bisulfite solution (ratio 1:10 *w/v*) and subjected to magnetic stirring for 4 h at room temperature. The mixture was homogenized in an ultra-turrax (T20 digital Ultra-Turrax), then filtered through a 100 mesh, after which the residue was washed thoroughly with distilled water. The filtrate was left for 30 min and the supernatant was decanted; the starch residue was resuspended in distilled water, then centrifuged at 3000× *g* for 10 min to precipitate the starch. The mango kernel starch was dried in a hot air tray dryer at 40 °C for 12 h.

Chemical Composition

Moisture, ash and fat content were estimated according to the standard procedure AOAC [27]. Moisture was determined by heating at 105 °C to a constant weight (925.10). Lipids were extracted by Soxhlet using petroleum ether (945.16). The ash content was determined by complete incineration in a muffle furnace at 550 °C (923.03). The amylose content was determined using the Morrison and Laignelet [28] colorimetric method; the readings were taken at 620 nm on a Genesys 10S UV-vis spectrophotometer (Thermo Fischer Scientific Inc., Waltham, MA, USA), which was also used to produce a straight-line standard curve obtained from pure amylose solutions. The difference calculated amylopectin content to 100% of amylose content.

2.5. Formulation of Emulsion Gels (EGs)

A 2^3 factorial design evaluated the percentage of canola oil (10, 20 and 30% *w/w*) and mango kernel starch (0.5, 1.0 and 1.5% *w/w*), obtaining 12 samples, as shown in Table 1. The EG samples were carried out following the methodology used by Shi [29] with modifications. Mango kernel starch and CMC blends (3% *w/w*) were initially dispersed in deionized water for 4 h at 25 °C to solubilize and form the aqueous phase; after that, Tween 80 was added as a surfactant (0.5% *w/w*). The oil phase was prepared to mix canola oil with 1% *w/w* of mango peel extract using an ultrasonic bath at a frequency of 25 KHz for 10 min; the percentages of extract were chosen considering the final concentration of TPC in all emulsions formulated, according to health recommendations (800 mg/100 g of selected foods or for nutritional supplements; 50 mg/day isoflavones or 100–300 mg/day grape seed extracts rich in proanthocyanidins) [30,31]. Oil-in-water emulsions were prepared by homogenizing oil in an aqueous phase in a rotor-stator homogenizer Ultra Turrax (IKA digital T20 Ultra Turrax, Germany) at 8000 rpm for 3 min. Then, the emulsions were heated

to 80 °C for 5 min and, meanwhile, shearing was applied using an overhead stirrer. The sample was cooled to 4 °C and the gels were covered with a catering film to reduce water evaporation. All samples were stored for 48 h at 4 °C until analysis.

Table 1. Sample code and formulation of carboxymethylcellulose/mango starch emulsion gel with mango peel extract.

Sample Code	Canola Oil %	Water %	Mango Starch %	CMC %	Tween 80 %	Mango Peel Extract %
EG10-MS	10	90	0	3	0.5	1
EG10-MS0.5	10	90	0.5	3	0.5	1
EG10-MS1.0	10	90	1	3	0.5	1
EG10-MS1.5	10	90	1.5	3	0.5	1
EG20-MS	20	80	0	3	0.5	1
EG20-MS0.5	20	80	0.5	3	0.5	1
EG20-MS1.0	20	80	1	3	0.5	1
EG20-MS1.5	20	80	1.5	3	0.5	1
EG30-MS	30	70	0	3	0.5	1
EG30-MS0.5	30	70	0.5	3	0.5	1
EG30-MS1.0	30	70	1	3	0.5	1
EG30-MS1.5	30	70	1.5	3	0.5	1

2.5.1. Color Measurement

The colorimeter measured the color parameters lightness (L*), red–green color (a^*) and yellow–blue color (b^*) of EGs. Whiteness index (WI) and color variation (ΔE^*) were calculated by Equations (1) and (2), respectively [23,32]:

$$WI = 100 - \left[(100 - L^*)^2 + a^{*2} + b^{*2}\right]^{0.5} \quad (1)$$

$$\Delta E^* = \left[(\Delta L^*)^2 + (\Delta a^*)^2 + (\Delta b^*)^2\right]^{0.5} \quad (2)$$

2.5.2. Dynamic Rheological Characterization

Rheological measurements of EG were performed to evaluate the viscoelastic properties of the emulsion gels employing a modular advanced rheometer system Mars 60, Haake (Thermo Scientific, Karlsruhe Germany), equipped with a cone-plate geometry (1°; 35 mm diameter and 0.053 mm GAP). A stress amplitude sweep test was carried out within the range of 0.01–1000 Pa and with an angular frequency at 1 Hz to determine the linear viscoelastic regime. After that, the frequency sweep was performed at 1 Pa to keep the stress in the linear viscoelastic regime, within the range of 0.01–100 rad·s^{-1}.

Analysis of rheological parameters included storage (G') and loss (G'') modulus and complex viscosity (η^*). Frequency curves (G' and G'' versus ω) were fitted to power-law using Equations (3) and (4) [33]:

$$G' = k'.\,\omega^{n'} \quad (3)$$

$$G'' = k''.\,\omega^{n''} \quad (4)$$

in these expressions, the magnitude of G' and G'' are represented by the values of k' and k'' coefficients and the exponents n' and n'' are the slopes representing the relationship between modulus and frequency, i.e., when the exponent value is far from zero, it represents a characteristic behavior of a weak gel [29].

2.5.3. Creep and Recovery Test

Creep recovery tests for EGs were carried out by subjecting the samples to a constant stress amplitude (1 Pa) for 180 s at 25 °C, followed by stress release and recovery for 180 s

by decreasing the stress to zero. The creep-recovery compliance (J) was calculated with Equation (5):

$$J(t) = \frac{\gamma(t)}{\tau_0} \quad (5)$$

The creep recovery percentages of the emulsion gels were then calculated based on Equation (6):

$$\%\ recovery = \frac{J_m - J_e}{J_m} \times 100 \quad (6)$$

where $J(t)$ (Pa^{-1}) is creep compliance, γ is the measured strain, t is time, τ_0 is the constant applied shear stress, J_m (Pa^{-1}) is the maximum creep and J_e (Pa^{-1}) is the equilibrium creep compliance after recovery.

Creep curves were analyzed according to the Burgers model with one Kelvin–Voigt element (Equation (7)) [34]:

$$J = \frac{1}{G_1} + \frac{1}{G_2}\left(1 - exp\left(\frac{-t}{\lambda_{ret}}\right)\right)\frac{t}{\mu_0} \quad (7)$$

where J is compliance, t is the time, G_1 is $1/J_1$, which is the time-independent elastic jump in the creep curve, λ_{ret} is the retardation time of Kelvin–Voight element and μ_0 is Newtonian viscosity. In other words, the compliance, J, in the Burgers equation is the sum of instantaneous elastic response, a viscoelastic (delayed elastic) component and the unrecovered viscous flow.

2.5.4. Optical Microscopy

A primo Star optical microscope (Carl Zeiss Primo Star Microscopy GmbH, Jena, Germany) with a 100× magnification lens was used to observe the internal distribution and droplet size of the emulsions (ca. 50 µL). A DCMC310 digital camera with Scope Photo software (Version 3.1.615) from Hangzhou Huaxin Digital Technology Co., Ltd., Zhejiang, China, attached to the optical microscope captured images.

2.6. Statistical Analysis

Data were analyzed with a unidirectional ANOVA using the Statgraphics software (version centurión XVI) to determine statistically significant differences ($p < 0.05$) between samples. All tests were performed in triplicate.

3. Discussion

3.1. Mango Peel Extract

Mango peel extracts had extraction yields (g mango peel extract/g mango peel × 100) of 11.35 ± 2.05% *w/w*. Ultrasound-assisted extraction causes bubble bursting and chaos near the surface, improving mass transfer, which can accelerate swelling and hydration of plant tissues and increase the extraction rate [35,36]. The yield values obtained in this study were higher than those extracts reported by Zou [37], showing extracts isolated by UAE using a two-cycle irradiation methodology with a lower concentration of ethanol (5.84%). Besides, similar results were reported by Dorta et al. [38] with ethanolic mango peel extracts using a solid–liquid extraction with microwave-assisted extraction for 60 min (6.0–16%) and higher yields have been found when applying sequential extraction with water; ethanol as solvent and 8 cycles of extraction (67%) [39]. This variation in yield extraction can be attributed to the method used and the different compositions presented in each variety of mango [40].

The TPC content of the extract was 294.60 ± 0.03 mg GAE/100 g of extract. Other results in mango peel of different varieties have been reported with values in a wide range, from 205.08 to 7953 mg GAE/g, [41–43], which are within the results reported in this work. Furthermore, the antioxidant activity of the extract is determined by the reduction of the radical ABTS, which presented EC_{50} values of 17.441 ± 0.21 and 436.77 ± 5.30 µMol Trolox/g

of extract, which are strongly linked to the bioactive compounds found in each extract studied and their ability as antioxidants by the reduction of the ABTS radical [44]. Then, different phenolic compounds were identified in the extract; Figure 1 reflects the existence of bioactive compounds in mango peel extracts, such as pyrogallol (12.27%), melezitose (2.29%), succinic acid (0.03%), $\gamma-$tocopherol (1.09%), campesterol (0.93%), stigmasterol (1.35%) and lupeol (2.55%) and vitamin A (Retinyl palmitate) (0.07%) and vitamin E (5.17%) (Table A1), demonstrated the potential functional properties of this extracts, due to their phenolic compounds being related to health benefits [45] and biological properties [46].

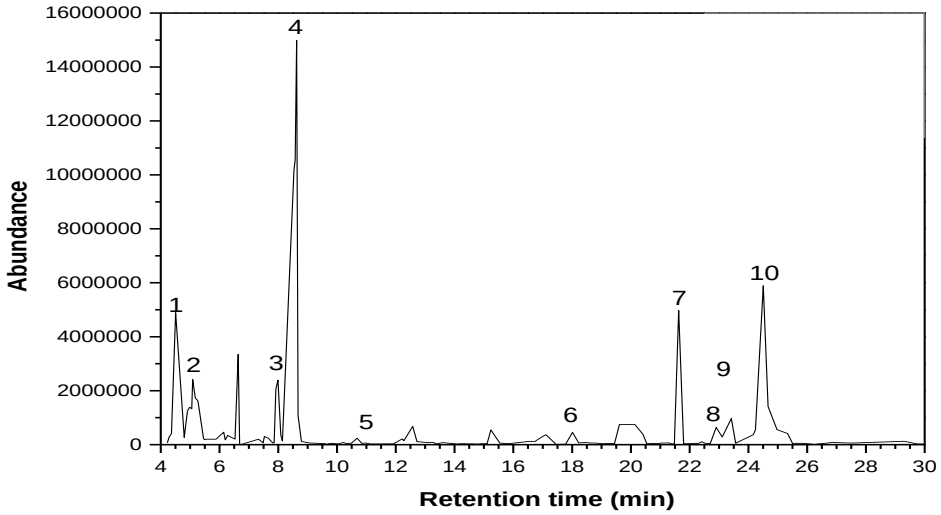

Figure 1. Chromatogram of mango peel extracts. (1) Pyrogallol (R.T., 4.51); (2) Melezitose (R.T., 5.08); (3) Succinic acid (R.T., 7.86); (4) Linolelaidic acid (R.T., 8.53); (5) Vitamin A (Retinyl palmitate) (R.T., 10.97); (6) $\gamma-$ tocopherol (R.T., 20.41); (7) Vitamin E (R.T., 21.63); (8) Campesterol (R.T., 22.91); (9) Stigmasterol (R.T., 23.42); (10), $\gamma-$sitosterol (R.T., 24.51).

3.2. Mango Kernel Starch

Mango kernel starch showed extraction yields of 59.51 $\pm$ 1.35% *w/w*, according to mango kernel starches of Indian cultivars (60.12 $\pm$ 0.53%) [47] and unripe mango kernel starch (48.79 $\pm$ 1.66%) [48]. Obtained starch presented low moisture and fat content with values of 8.21 $\pm$ 1.54 g of water/100 g and 0.34 $\pm$ 0.07 g/100 g, respectively, compared with starch from cereals and tubers [49,50]. The amount of ash (0.29 $\pm$ 0.09 g/100 g) was based on the starch content isolated from unconventional sources such as African breadfruit kernel and mango kernel [51].

The content of amylose, amylopectin, fat and ash is decisive in the structural and functional characteristics of starch, affecting some particularly useful properties in the food industry, such as the solubility and binding characteristics of gelatinization and texture [52]. In the current study, the amylose content was 27.28 $\pm$ 0.05%, classified as normal starch (amylose values between 20 and 35%) [53], which agrees with previously reported values (24.1–33.6%) of mango kernel starch from three mango cultivars [54,55] and is closer to convection starches, i.e., yam, sweet potato, cassava, potato and corn (19.6–28.3%) [56]. The amylose content is essential for the production of resistant starches, since starches with a high amylose content have a greater retrograde capacity and, therefore, greater formation of resistant starches (more resistant gels) [57]; this indicates that the efficiency of the starch extraction process is close to 100% and that the remnants of other nutrients are embedded within the starch matrix. The isolation process produced low-fat starch, reducing the probability of rancidity [58].

3.3. Emulsion Gel (EG)

The visual appearance of the emulsion gels was evaluated as a function of storage time (15 days). On the first day, all freshly prepared gels represented white color, indicating

that the green color of mango peel extracts did not change the appearance of the sample, verified by assessing the color parameters.

The gels stabilized with CMC mango starch did not flow when placed in reverse, indicating that firm emulsions were formed (Figure 2). However, the other gels did not form enough solid gels due to a certain fluidity at the bottom, which was similar to previous reports [59]. However, all emulsion gels were stable for 15 days, indicating the good stabilizing capacity of CMC-mango kernel starch; it can provide bioactive activity from polyphenols as antioxidants and antimicrobials in most semisolid foods that have an emulsion structure.

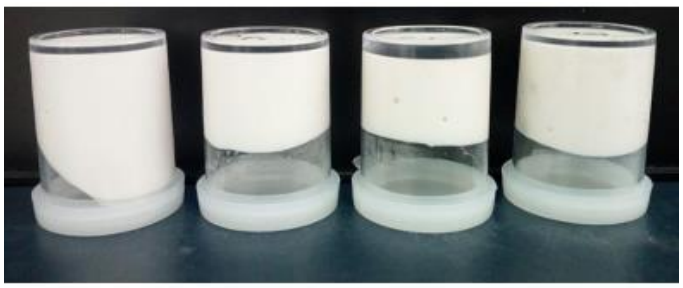

(**a**) (**b**) (**c**) (**d**)

Figure 2. The visual appearance of EG with 20% of oils: (**a**) 0% of CMC (EG20-MS), (**b**) 0.5% of CMC (EG20-MS0.5), (**c**) 1.0% of CMC (EG20-MS1.0) and (**d**) 1.5% of CMC (EG20-MS1.5).

To evaluate the influence of formulations on the visual appearance of the sample, the analysis of the parameters was performed (Table 2). In general, the highest lightness (L* > 71) and whiteness index (WI > 59) are associated with the white color of samples, corroborating that the incorporation of mango peel extracts did not change the emulsion gel appearance. This is an advantage in the use of polyphenolic extracts due to the preservation of sensory attributes such as color, in terms of darkening of the product, considering that this parameter is essential in the development of fat analogs, since it is one of the main factors that determine consumer acceptance.

Table 2. Color parameters obtained for EG-m formulations of carboxymethylcellulose/mango starch emulsion gels with 1% *w/w* of mango peel extracts. L*, lightness; WI, whiteness index; ΔE, color variation.

Sample Code	L*	WI	ΔE
EG10-MS	90.79 ± 3.85^{ab}	83.92 ± 0.29^{a}	-
EG10-MS0.5	77.49 ± 6.17^{def}	75.56 ± 5.91^{acd}	14.57 ± 5.10^{ab}
EG10-MS1.0	71.18 ± 2.36^{fg}	68.88 ± 0.88^{de}	20.09 ± 2.56^{abc}
EG10-MS1.5	74.12 ± 12.26^{efg}	70.95 ± 12.22^{cde}	17.37 ± 11.62^{ab}
EG20-MS	83.09 ± 0.53^{cd}	79.39 ± 0.60^{ab}	-
EG20-MS0.5	78.42 ± 0.77^{cde}	77.58 ± 0.80^{abc}	7.48 ± 0.49^{cd}
EG20-MS1.0	74.41 ± 1.76^{efg}	71.96 ± 2.64^{cde}	9.50 ± 1.77^{cd}
EG20-MS1.5	71.34 ± 0.48^{efg}	66.12 ± 0.66^{ef}	13.47 ± 0.65^{bcd}
EG30-MS	60.99 ± 1.15^{h}	59.72 ± 0.96^{f}	-
EG30-MS0.5	96.01 ± 0.24^{a}	93.58 ± 0.33^{g}	32.00 ± 0.21^{e}
EG30-MS1.0	70.08 ± 1.41^{g}	68.78 ± 1.63^{de}	6.04 ± 1.53^{d}
EG30-MS1.5	85.32 ± 0.61^{bc}	$\pm 0.34^{a}$	21.15 ± 0.59^{a}

Data are expressed as mean ± standard deviation. Different letters in the same column express statistically significant differences ($p < 0.05$).

The addition of starch decreased lightness (L*) and whiteness index (WI) ($p < 0.05$) and the percentage of the oil phase in samples with CMC (EG10-MS, EG20-MS and EG30-MS) decreased L* and WI values; nevertheless, in samples with CMC and mango starch, it increased it. The changes in the WI of the samples can be related to changes in the structure,

resulting in different changes in light scattering. Several authors observed similar results, reporting that the addition of corn-modified starch and nanocrystals of corn starch affected light scattering in the emulsions [60,61]. Then, emulsion gels with mango peel extract could be an interesting alternative for the development of products due to the influence of color.

3.4. Rheological Properties

The rheological behavior of the emulsion gel was evaluated through oscillation measurements. The storage modulus (G') was greater than the loss modulus (G'') throughout the frequency range studied (Figure 3), which means that the elastic character was predominant, compared to the viscous component, or that the deformation in the linear range was essentially elastic or recoverable; this conduct has been evidenced to be characteristic in systems with gel-like behavior which present formation of networks well-developed in their structure [62].

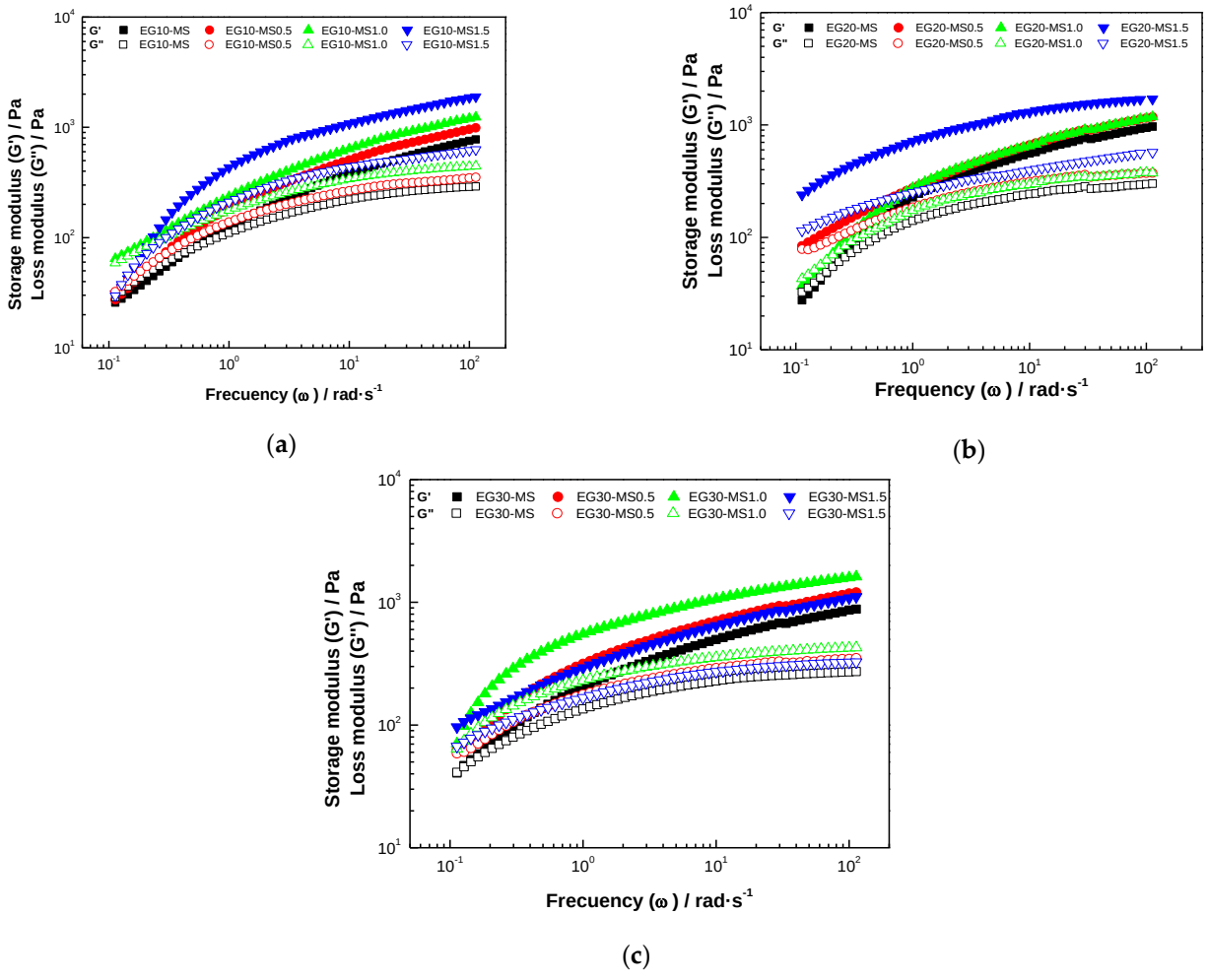

Figure 3. The storage modulus (G') and modulus (G'') as a function of frequency (ω) of carboxymethyl cellulose/mango-starch emulsion gels with 1% *w/w* of mango peel extracts at (**a**) 10%, (**b**) 20% and (**c**) 30% of canola oil (cv < 0.05%).

An increase in the concentration of mango kernel starch resulted in higher values of G' and G'', so the gel strength was higher when 1.5% of starch was added. Therefore, it can be considered that the network formed by CMC and starch improved the gel strength of the emulsion and inferred that the intermolecular interactions were more complex between both polymers, given the contribution to the rheological character originating in the complexity and stability associated with the mixture of these polymers [63]. However, samples with higher oil content (30%) and 1.0% of starch (EG30-MS1.0) presented higher

G' values and developed elasticity features, which means that this formulation had the strongest gel transformation attributed to complex interactions of components.

The power-law parameters (k', k'', n' and n'') presented a high correlation coefficient ($R^2 \geq 0.88$), indicating that the power-law model can accurately describe the behavior of the G' and G'' modules (Table 3). k' was greater in samples with higher oil percentage ($p < 0.05$) related to the increase in the number of particles per unit volume, which reduces the spacing between the particles, resulting in enhanced interactions and the creation of bounds creation between droplets and with the reinforcement of the emulsion gel structure, while k'' did not change with the percentage of oil ($p > 0.05$). In the same way, k' and k'' increased with the percentage of starch ($p < 0.05$); these results are in accord with other published works [64], when the rheological properties of EGs are strongly dependent on the intrinsic properties of the mango kernel starch.

Table 3. Viscoelasticity parameters for carboxymethyl cellulose/mango-starch emulsion gels with 1% *w/w* of mango peel extracts.

Sample Code	k' Pa·s^n	n'	R^2	k'' Pa·s^n	n''	R^2	$\eta^*_{(\omega=1 rad \cdot s^{-1})}$ Pa·s
EG10-MS	147.32 ± 4.68 ^{a}	0.36 ± 0.01 ^{a}	0.98	114.16 ± 3.83 ^{a}	0.22 ± 0.01 ^{ab}	0.92	167.2 ± 2.34
EG10-MS0.5	205.93 ± 6.92 ^{b}	0.34 ± 0.01 ^{a}	0.97	139.20 ± 4.78 ^{b}	0.22 ± 0.01 ^{ab}	0.92	196.2 ± 2.52
EG10-MS1.0	267.13 ± 7.58 ^{d}	0.34 ± 0.02 ^{a}	0.98	181.60 ± 5.44 ^{c}	0.21 ± 0.02 ^{bc}	0.93	219.4 ± 1.24
EG10-MS1.5	463.54 ± 18.61 ^{g}	0.31 ± 0.01 ^{b}	0.95	215.90 ± 7.94 ^{d}	0.24 ± 0.01 ^{a}	0.93	336.8 ± 2.43
EG20-MS	243.69 ± 9.20 ^{c}	0.31 ± 0.01 ^{b}	0.96	134.82 ± 4.73 ^{b}	0.19 ± 0.01 ^{bcd}	0.88	245.6 ± 1.65
EG20-MS0.5	257.61 ± 3.38 ^{cd}	0.35 ± 0.02 ^{a}	0.96	184.36 ± 5.02 ^{c}	0.17 ± 0.01 ^{ef}	0.90	331.8 ± 2.63
EG20-MS1.0	289.51 ± 10.14 ^{e}	0.31 ± 0.01 ^{b}	0.96	167.06 ± 5.66 ^{e}	0.20 ± 0.01 ^{bcd}	0.89	294.1 ± 1.74
EG20-MS1.5	715.54 ± 18.52 ^{i}	0.21 ± 0.01 ^{c}	0.94	244.40 ± 3.19 ^{f}	0.19 ± 0.01 ^{cde}	0.97	439.5 ± 1.52
EG30-MS	220.96 ± 6.71 ^{b}	0.31 ± 0.02 ^{b}	0.97	132.38 ± 4.00 ^{b}	0.18 ± 0.02 ^{def}	0.89	267.4 ± 2.78
EG30-MS0.5	307.98 ± 6.92 ^{ef}	0.28 ± 0.01 ^{d}	0.98	165.51 ± 3.94 ^{e}	0.17 ± 0.01 ^{ef}	0.91	341.6 ± 1.42
EG30-MS1.0	325.45 ± 9.60 ^{f}	0.29 ± 0.01 ^{bd}	0.97	171.24 ± 4.98 ^{e}	0.17 ± 0.01 ^{ef}	0.89	599.4 ± 1.92
EG30-MS1.5	541.00 ± 16.16 ^{h}	0.25 ± 0.01 ^{e}	0.95	218.12 ± 5.90 ^{d}	0.16 ± 0.01 ^{f}	0.89	748.8 ± 1.30

Different letters in the same column express statistically significant differences ($p < 0.05$).

n' and n'' were found in the range of 0.21–0.36 and 0.16–0.24, respectively, which corroborates that both modules presented a slight dependence on the frequency studied. In all cases where n' and n'' values were close to zero, representing a physical gel [65]. The values obtained were closer to those reported by Quig Li [66] (0.06–0.22) for emulsion gels with Glycyrrhizic acid mono ammonium salt and Lu et al. [67] for hydrogels oh chitosan (0.2–0.22). Subsequently, EGs presented a more elastic behavior with higher starch and oil content.

In the entire frequency range, all samples showed a linear decrease in complex viscosity $|\eta^*|$ (Figure 4), which corresponds to the behavior of a viscoelastic solid with a gel-like structure [68]; this is due to the rupture of the droplet clusters under the action of the applied deformation in the frequency range under study. As can be seen in Table 3, a high percentage increase η^* (Figure A1), moving upward to higher viscosity, indicates that the network structure was enhanced, as oil droplets contributed to the formation of ion gel networks, which may be the reason for the increase in the viscosity of the emulsion gels [62]. In addition, the samples with higher mango kernel starch content presented the highest complex viscosity values, associated with the interaction between starch molecules which covering adjacent oil droplets; however, these interactions were weak [69].

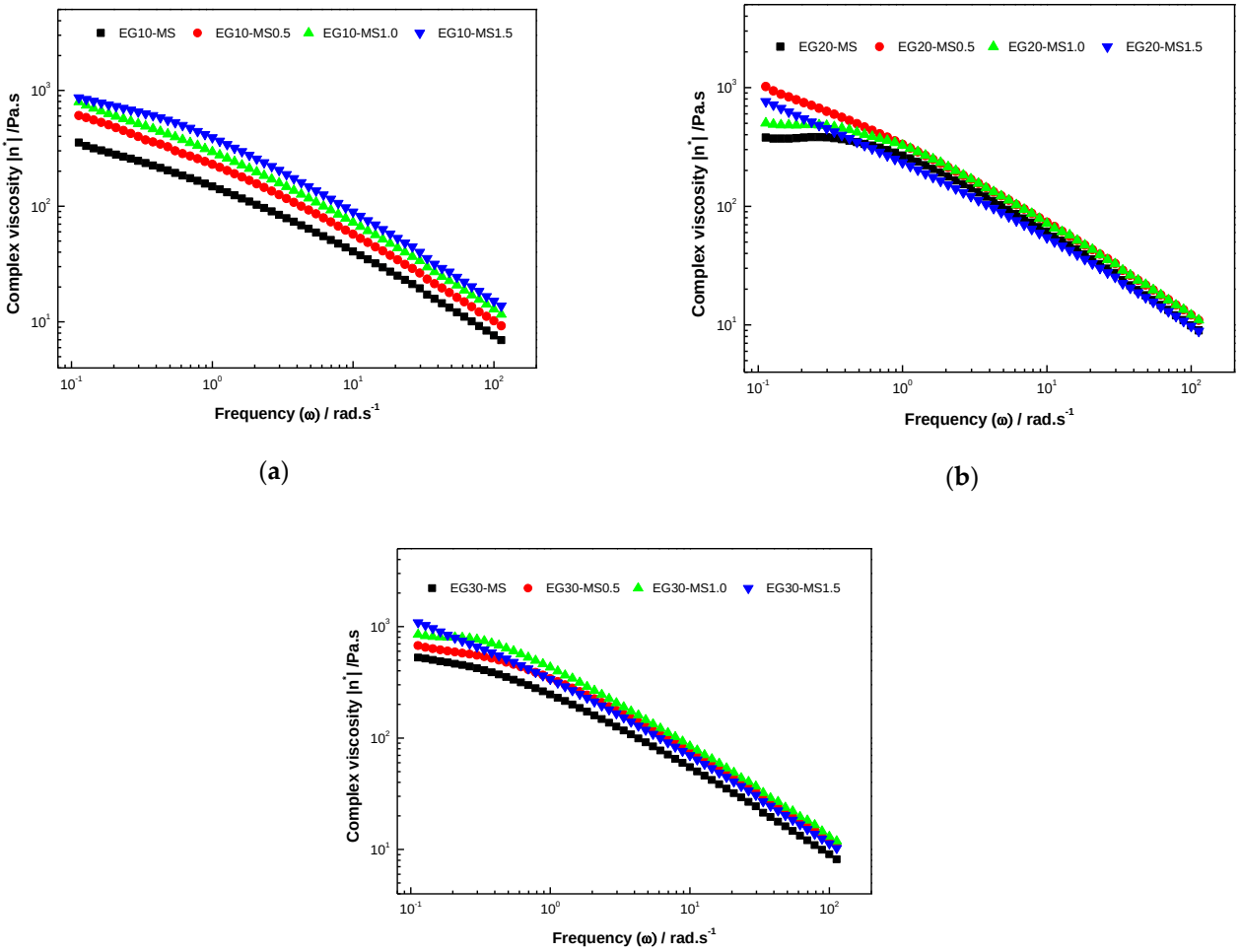

Figure 4. Complex viscosity as a function of frequency (ω) of carboxymethyl cellulose/mango-starch emulsion gels with 1% *w/w* of mango peel extracts at (**a**) 10%, (**b**) 20% and (**c**) 30% of canola oil.

Creep and Recovery

The creep-recovery tests can be used to evaluate the transient behavior of the viscoelastic properties of emulsion gels. When a viscoelastic material is subjected to prompt and constant stress, the deformation rises over time and the consequent elimination of stress results in a reduction in the strain. This behavior is directly related to the viscoelastic features of the material, which might or might not reach zero deformation over time [70].

Creep-recovery data compliance (J) is shown in Figure 4. The extensional creep measurement curves of the emulsion gel exhibited a behavior characteristic of viscoelastic material, although presenting different degrees of viscoelasticity; the maximum compliance data expressed the peak deformation in the completion of the creep phase (180 s), while the relative recovery was the deformation recovered at the end of the recovery phase, divided by the peak deformation (180–360 s). A lower peak deformation specifies a stiffer structure with lower flowability.

The compliance (J) of emulsion gels (Figure 5) decreased with the addition of an oil percentage from 10% to 20% (Figure 5a,b), but, in the case with 30% (Figure 5c), the compliance increased again; these changes are related to a three-dimensional cross-linked and continuous gel matrix by molecular interaction, leading to a change in viscoelastic properties [71]. Moreover, with the increment in the percentage of mango kernel starch, the compliance (J) of the emulsion gels decreased, confirming the viscoelastic characteristics given by the content of mango kernel starch and oil fraction mentioned in the power-

law analysis. In addition, after the emulsion gel stress was released, the deformation of the emulsion gel could be restored due to the good viscoelasticity of the emulsion gel. This type of recoverability benefits foods subjected to various stresses during complex applications [72].

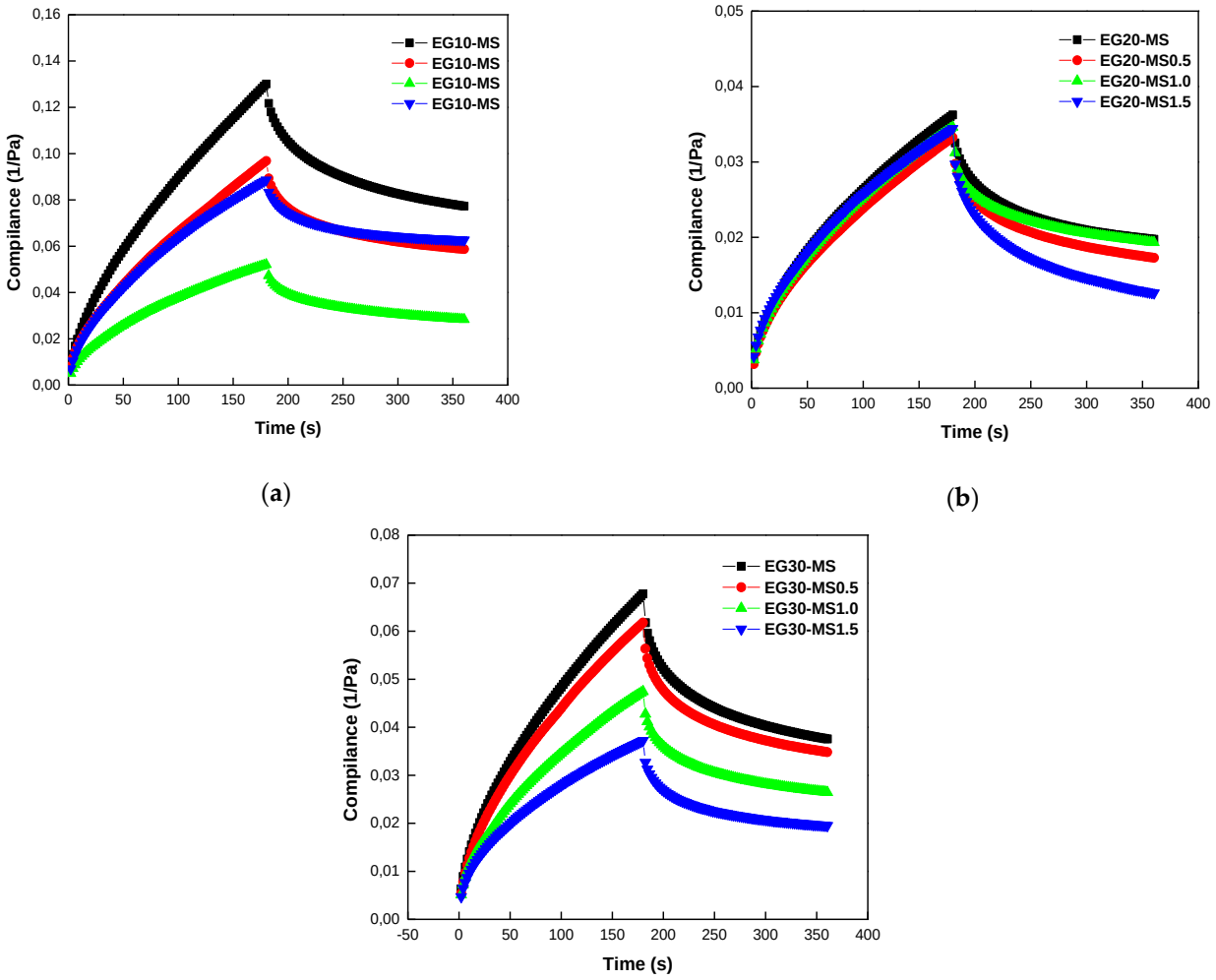

Figure 5. Creep and recovery curves of carboxymethyl cellulose/mango-starch emulsion gels with 1% *w/w* of mango peel extracts at (**a**) 10%, (**b**) 20% and (**c**) 30% of canola oil.

As shown in Table 4, the Burgers model fits very well with the experimental data ($R^2 > 0.96$). Creep compliance decreased with increasing canola oil proportion from 10% to 20% *w/w*, indicating the formation of a stronger gel emulsion structure with increasing canola oil proportion. However, as the oil proportion increased from 20% to 30% (*w/w*), the creep compliance increased, indicating a weaker emulsion gel structure. The retardation time (λ_{ret}) was different for oil content ($p < 0.05$) but not for starch ($p > 0.05$); this suggests that the treatment with high oil content presented a high-speed transition between the elastic and viscous regimes during deformation. The μ_o value represents the viscous behavior of the gel network and greater μ_o values show that the viscous element of these gels would be higher, and the gels would show less flowability.

Table 4. Burgers model parameters obtained from carboxymethyl cellulose/mango-starch emulsion gels with 1% *w/w* of mango peel extracts.

Sample Code	G_1 Pa	G_2 Pa	λ_{ret} s	$\mu_o \times 10^3$ Pa.s	R^2	Recovery %
EG10-MS	21.02 ± 0.72 ^{b*}	17.98 ± 0.35 ^{a*}	103.51 ± 4.93 ^{b*}	1.8 ± 100.56 ^{a*}	0.98	38.53 ± 2.91 ^{b*}
EG10-MS0.5	29.11 ± 1.67 ^{ab*}	25.56 ± 0.89 ^{ab*}	109.38 ± 8.91 ^{b*}	2.7 ± 130.81 ^{a*}	0.99	39.29 ± 0.11 ^{ab*}
EG10-MS1.0	43.26 ± 2.60 ^{a*}	42.92 ± 0.80 ^{a*}	160.42 ± 3.65 ^{a*}	6.8 ± 330.22 ^{b*}	0.97	47.27 ± 2.41 ^{a*}
EG10-MS1.5	23.98 ± 1.01 ^{b*}	31.16 ± 1.50 ^{a*}	104.24 ± 5.29 ^{b*}	3.1 ± 184.74 ^{a*}	0.98	36.94 ± 1.33 ^{b*}
EG20-MS	64.59 ± 1.17 $^{ab*+}$	64.28 ± 2.15 $^{b+}$	158.68 ± 6.35 $^{a+}$	9.6 ± 330.50 $^{a+}$	0.96	48.23 ± 3.86 ^{a*}
EG20-MS0.5	75.57 ± 1.25 $^{a+}$	66.10 ± 1.87 $^{a+}$	157.00 ± 5.25 $^{a+}$	9.8 ± 235.25 $^{a+}$	0.96	50.64 ± 3.73 ^{a*}
EG20-MS1.0	51.97 ± 0.90 $^{b+}$	82.96 ± 0.67 $^{a+}$	133.50 ± 7.25 $^{a+}$	10.5 ± 625.35 $^{a+}$	0.98	29.78 ± 2.01 ^{b*}
EG20-MS1.5	59.69 ± 0.93 $^{b+}$	57.91 ± 1.06 $^{a+}$	183.40 ± 8.05 $^{a+}$	10.12 ± 231.22 $^{a+}$	0.96	48.65 ± 4.50 ^{a*}
EG30-MS	33.70 ± 1.92 $^{a-}$	31.67 ± 1.02 ^{c*}	140.47 ± 2.72 $^{a*+}$	4.4 ± 197.28 $^{bc-}$	0.97	45.03 ± 0.63 ^{a*}
EG30-MS0.5	35.67 ± 2.81 $^{a-}$	35.11 ± 1.27 ^{c*}	124.19 ± 2.16 $^{a*+}$	4.3 ± 250.65 $^{c-}$	0.98	41.39 ± 3.19 ^{a*}
EG30-MS1.0	48.15 ± 2.25 $^{a-}$	47.34 ± 0.43 ^{b*}	183.75 ± 1.71 $^{a*+}$	8.6 ± 435.00 $^{ab-}$	0.97	50.93 ± 9.45 ^{a*}
EG30-MS1.5	55.70 ± 2.75 $^{a-}$	59.36 ± 2.00 ^{a*}	182.01 ± 2.26 $^{a*+}$	10.2 ± 692.89 $^{a-}$	0.98	49.92 ± 3.36 ^{a*}

Different letters in the same columns express statistically significant differences ($p < 0.05$) for starch. Different symbols in the same columns express statistically significant differences ($p < 0.05$) for oil.

After the applied stress was released, strain recovery occurred because of the good viscoelastic properties of the emulsion gels. This recovery is beneficial for food products that experience various forces in complex application processes. A relation with % recovery could not be established, although significative differences ($p < 0.05$) were obtained for starch concentration in samples with 10 and 20% of oils but was similar ($p > 0.05$) in samples with 30%; the starch content did not affect the % recovery. The increase in recovery rate may be due to the stronger network structure of the emulsion gel at higher solid-phase concentrations [73]. As expected, part of the deformation generated by the loading phase was not recovered because of the viscoelastic character of the emulsion gels.

3.5. Microstructural Properties

In Figure 6, optical microstructure images show emulsion gels with an emulsion droplet-aggregated gel behavior, forming a network structure. The samples contained active fillers, which improved the chemical and physical affinity between the gel matrix and emulsion droplets [74]. Furthermore, at the lowest oil content, the emulsion droplets were dispersed throughout the gel network created by CMC and mango kernel starch, but left gaps between the droplets, leading to the formation of heterogeneous and unstable droplets with different droplet sizes.

The mean diameter size decreased with the percentage of oil and mango kernel starch; when the oil content increased, these gaps were filled because the number of droplets per unit of area in the gel matrix increased and they started to associate with each other, thus forming a three-dimensional network given by the successful integration of the droplets and the gel matrix. With the increasing concentration of mango kernel starch, the average droplet size of oil decreased in all cases, increasing contact points and improve the organization between emulsion droplets [75]. This contribute to the increase of G' and the viscosity of the emulsion gel, since, with larger droplet size, the droplets become unstable, causing the decrease in the previously mentioned rheological parameters [76]; this was verified by evaluating the rheological behavior (see Section 2.5). In addition, the emulsion type was determined by performing the dropping test, in which a droplet of the formed emulsion was added to both the water and oil phases separately. If the droplet was well dispersed in water, then the emulsion type was defined as oil-in-water and the same rule was also applied to droplets dispersed in oil [77].

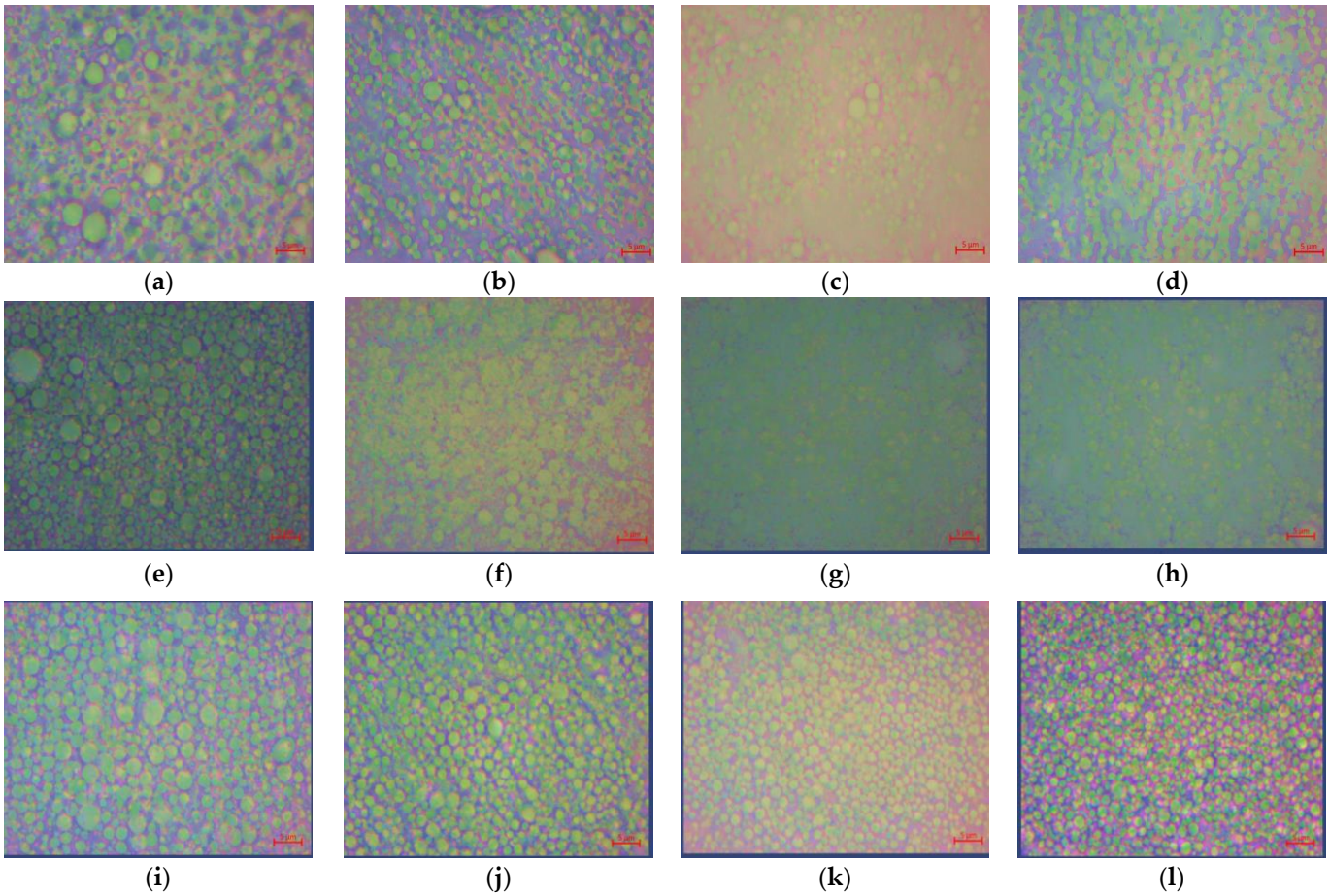

Figure 6. Microstructure and mean diameter size of carboxymethyl cellulose/mango-starch emulsion gels with 1% *w/w* of mango peel extracts. (**a**) EG10-MS (4.64 ± 0.83 μm), (**b**) EG10-MS0.5 (2.52 ± 0.21 μm), (**c**) EG10-MS1.0 (1.72 ± 0.39 μm), (**d**) EG10-MS1.5 (1.30 ± 0.26 μm), (**e**) EG20-MS (3.87 ± 0.18 μm), (**f**) EG20-MS0.5 (3.48 ± 0.69 μm), (**g**) EG20-MS1.0 (2.94 ± 0.34 μm), (**h**) EG20-MS1.5(1.76 ± 0.11 μm), (**i**) EG30-MS (3.92 ± 0.23 μm), (**j**) EG30-MS0.5 (2.75 ± 0.25 μm), (**k**) EG30-MS1.0 (1.93 ± 0.26 μm) and (**l**) EG30-MS1.5 (1.66 ± 0.06 μm).

4. Conclusions

Emulsion gels loading with bioactive mango peel extracts (pyrogallol, melezitose, succinic acid, $\gamma-$tocopherol, campesterol, stigmasterol, lupeol, Retinyl palmitate and vitamin E) were stabilized with blends of CMC and mango kernel starch (27.28 ± 0.05% of amylose). The characterization of emulsion gels revealed high gel strength and viscosity, with potential functional properties, due to the incorporation of extracts with antioxidant properties, as an alternative for the elaboration of products, considering that the green color of mango peel extracts did not change the appearance of the sample.

The rheological behavior revealed that the storage modulus (G') was greater than the loss modulus (G'') throughout the frequency range studied, which means that deformation in the linear range is essentially elastic or recoverable. In addition, the strain recovery of samples occurred because of the good viscoelastic properties of the samples. Then, the microstructure of emulsion gels exposed droplets sizes less than 5 μm, contributing to the stability of products. This work could facilitate designing a novel emulsion gel to develop fortified food products with nutrients or bioactive compounds.

Author Contributions: Conceptualization, L.M.-G., S.E.L.-R., E.T.-F., S.E.Q. and L.A.G.-Z.; methodology, L.M.-G., S.E.L.-R., S.E.Q. and L.A.G.-Z..; software, L.M.-G. and S.E.L.-R.; validation, S.E.Q. and L.A.G.-Z.; formal analysis, L.M.-G., S.E.L.-R., E.T.-F., S.E.Q. and L.A.G.-Z.; investigation, L.M.-G., S.E.L.-R., S.E.Q. and L.A.G.-Z.; resources, E.T.-F., S.E.Q. and L.A.G.-Z.; writing—original draft preparation, L.M.-G., S.E.L.-R., E.T.-F., S.E.Q. and L.A.G.-Z.; writing—review and editing, S.E.Q. and L.A.G.-Z.; supervision, L.A.G.-Z.; project administration, L.A.G.-Z.; funding acquisition, S.E.Q., E.T.-F. and L.A.G.-Z. All authors have read and agreed to the published version of the manuscript.

Funding: This research was funded by MINCIENCIAS, grant number 110780864755.

Acknowledgments: The authors gratefully acknowledge the financial support from the Ministry of Science, Technology, and Innovation—MinCiencias (Contract: 368–2019; research project No. 110780864755) and Strengthening Plan for research groups from University of Cartagena-Resolution 01430-2019.

Conflicts of Interest: The authors declare no conflict of interest.

Appendix A

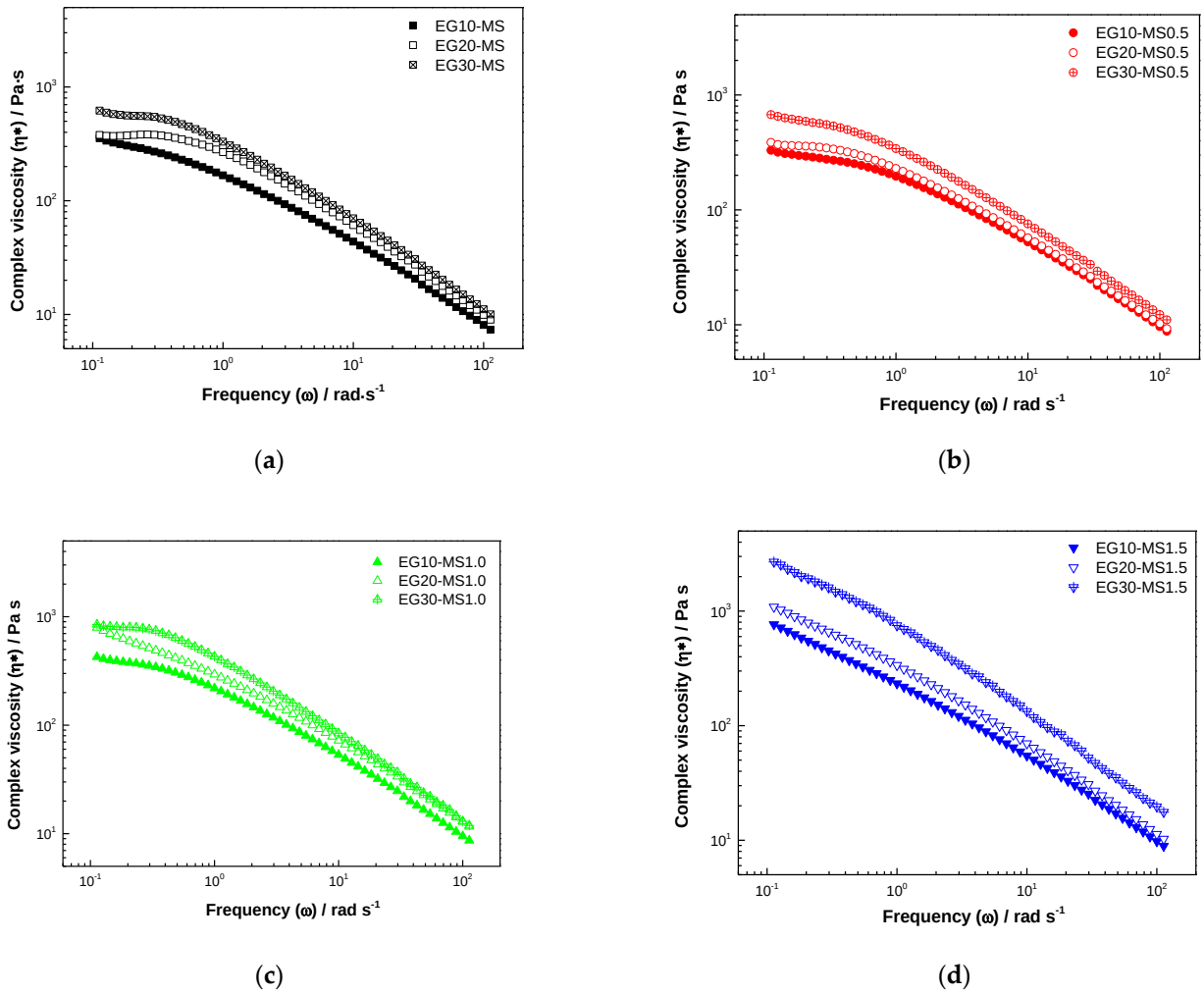

Figure A1. Complex viscosity of carboxymethyl cellulose/mango-starch emulsion gels with 1% *w/w* of mango peel extracts at (**a**) 0%, (**b**) 0.5%, (**c**) 1.0% and (**d**) 1.5% of starch.

Table A1. Chemical composition of mango peel extracts.

RT	Compounds	CAS	%A	%P
4.51	Pyrogallol	000087-66-1	12.27	95
5.08	Melezitose	000084-66-2	2.29	93
7.86	Succinic acid	1000353-45-5	0.03	78
8.53	Linolelaidic acid	000506-21-8	10.60	96
10.97	Vitamin A (Retinyl palmitate)	1000336-23-8	0.07	87
20.41	$\gamma-$tocopherol	007616-22-0	1.09	99
21.63	Vitamin E	000059-02-9	5.17	99
22.91	Campesterol	000474-62-4	0.93	99
23.42	Stigmasterol	000083-48-7	1.35	99
24.51	$\gamma-$sitosterol	000083-47-6	0.38	99
25.85	Lupeol	000545-47-1	2.55	95

RT, retention time; %A, area percentage; %P, probability.

References

1. Dickinson, E. Emulsion Gels: The Structuring of Soft Solids with Protein-Stabilized Oil Droplets. *Food Hydrocoll.* **2012**, *28*, 224–241. [CrossRef]
2. Balakrishnan, G.; Nguyen, B.T.; Schmitt, C.; Nicolai, T.; Chassenieux, C. Heat-Set Emulsion Gels of Casein Micelles in Mixtures with Whey Protein Isolate. *Food Hydrocoll.* **2017**, *73*, 213–221. [CrossRef]
3. Dos Santos Pereira, E.; Vinholes, J.R.; Camargo, T.M.; Nora, F.R.; Crizel, R.L.; Chaves, F.; Nora, L.; Vizzotto, M. Characterization of Araçá Fruits (Psidium Cattleianum Sabine): Phenolic Composition, Antioxidant Activity and Inhibition of α-Amylase and α-Glucosidase. *Food Biosci.* **2020**, *37*, 100665. [CrossRef]
4. Hou, J.-J.; Guo, J.; Wang, J.-M.; Yang, X.-Q. Effect of Interfacial Composition and Crumbliness on Aroma Release in Soy Protein/Sugar Beet Pectin Mixed Emulsion Gels. *J. Sci. Food Agric.* **2016**, *96*, 4449–4456. [CrossRef]
5. Cofrades, S.; Bou, R.; Flaiz, L.; Garcimartín, A.; Benedí, J.; Mateos, R.; Sánchez-Muniz, F.J.; Olivero-David, R.; Jiménez-Colmenero, F. Bioaccessibility of Hydroxytyrosol and N-3 Fatty Acids as Affected by the Delivery System: Simple, Double and Gelled Double Emulsions. *J. Food Sci. Technol.* **2017**, *54*, 1785–1793. [CrossRef] [PubMed]
6. Ma, L.; Wan, Z.; Yang, X. Multiple Water-in-Oil-in-Water Emulsion Gels Based on Self-Assembled Saponin Fibrillar Network for Photosensitive Cargo Protection. *J. Agric. Food Chem.* **2017**, *65*, 9735–9743. [CrossRef]
7. Quintana, S.E.; Llalla, O.; García-Zapateiro, L.A.; García-Risco, M.R.; Fornari, T. Preparation and Characterization of Licorice-Chitosan Coatings for Postharvest Treatment of Fresh Strawberries. *Appl. Sci.* **2020**, *10*, 8431. [CrossRef]
8. Quintana, S.E.; Llalla, O.; García-Risco, M.R.; Fornari, T. Comparison between Essential Oils and Supercritical Extracts into Chitosan-Based Edible Coatings on Strawberry Quality during Cold Storage. *J. Supercrit. Fluids* **2021**, *171*, 105198. [CrossRef]
9. Alañón, M.E.; Oliver-Simancas, R.; Gómez-Caravaca, A.M.; Arráez-Román, D.; Segura-Carretero, A. Evolution of Bioactive Compounds of Three Mango Cultivars (*Mangifera Indica* L.) at Different Maturation Stages Analyzed by HPLC-DAD-q-TOF-MS. *Food Res. Int.* **2019**, *125*, 108526. [CrossRef] [PubMed]
10. Quintana, S.E.; Salas, S.; García-Zapateiro, L.A. Bioactive Compounds of Mango (Mangifera Indica): A Review of Extraction Technologies and Chemical Constituents. *J. Sci. Food Agric.* **2021**, 1–7. [CrossRef]
11. Marcillo-Parra, V.; Anaguano, M.; Molina, M.; Tupuna-Yerovi, D.S.; Ruales, J. Characterization and Quantification of Bioactive Compounds and Antioxidant Activity in Three Different Varieties of Mango (*Mangifera Indica* L.) Peel from the Ecuadorian Region Using HPLC-UV/VIS and UPLC-PDA. *NFS J.* **2021**, *23*, 1–7. [CrossRef]
12. Fang, Z.; Bhandari, B. Encapsulation of Polyphenols—A Review. *Trends Food Sci. Technol.* **2010**, *21*, 510–523. [CrossRef]
13. Binks, B.P.; Lumsdon, S.O. Effects of Oil Type and Aqueous Phase Composition on Oil-Water Mixtures Containing Particles of Intermediate Hydrophobicity. *Phys. Chem. Chem. Phys.* **2000**, *2*, 2959–2967. [CrossRef]
14. Li, A.; Gong, T.; Hou, Y.; Yang, X.; Guo, Y. Alginate-Stabilized Thixotropic Emulsion Gels and Their Applications in Fabrication of Low-Fat Mayonnaise Alternatives. *Int. J. Biol. Macromol.* **2020**, *146*, 821–831. [CrossRef] [PubMed]
15. Herrero, A.M.; Ruiz-Capillas, C.; Pintado, T.; Carmona, P.; Jiménez-Colmenero, F. Elucidation of Lipid Structural Characteristics of Chia Oil Emulsion Gels by Raman Spectroscopy and Their Relationship with Technological Properties. *Food Hydrocoll.* **2018**, *77*, 212–219. [CrossRef]
16. Orgulloso-Bautista, S.; Ortega-Toro, R.; Alberto, L.; Zapateiro, G. Design and Application of Hydrocolloids from Butternut Squash (Cucurbita Moschata) Epidermis as a Food Additive in Mayonnaise-Type Sauces. *ACS Omega* **2021**, *6*, 5499–5508. [CrossRef]
17. Saha, D.; Bhattacharya, S. Hydrocolloids as Thickening and Gelling Agents in Food: A Critical Review. *J. Food Sci. Technol.* **2010**, *47*, 587. [CrossRef] [PubMed]
18. Copetti, G.; Grassi, M.; Lapasin, R.; Pricl, S. Synergistic Gelation of Xanthan Gum with Locust Bean Gum: A Rheological Investigation. *Glycoconj. J.* **1997**, *14*, 951–961. [CrossRef]
19. Nor Hayati, I.; Che Man, Y.B.; Tan, C.P.; Nor Aini, I. Droplet Characterization and Stability of Soybean Oil/Palm Kernel Olein O/W Emulsions with the Presence of Selected Polysaccharides. *Food Hydrocoll.* **2009**, *23*, 233–243. [CrossRef]

20. Sharma, B.R.; Dhuldhoya, N.C.; Merchant, S.U.; Merchant, U.C. Hydrocolloids: Efficient Rheology Control Additives. *Sci. Technol. Entrep.* **2007**, *2*, 1–9.
21. Dickinson, E. Hydrocolloids Acting as Emulsifying Agents—How Do They Do It? *Food Hydrocoll.* **2018**, *78*, 2–14. [CrossRef]
22. Mantelet, M.; Panouillé, M.; Boué, F.; Bosc, V.; Restagno, F.; Souchon, I.; Mathieu, V. Impact of Sol-Gel Transition on the Ultrasonic Properties of Complex Model Foods: Application to Agar/Gelatin Gels and Emulsion Filled Gels. *Food Hydrocoll.* **2019**, *87*, 506–518. [CrossRef]
23. Lastra-Ripoll, S.E.; Quintana-Martinez, S.E.; Garcia-Zapateiro, L.A. Rheological and Microstructural Properties of Xanthan Gum-Based Coating Solutions Enriched with Phenolic Mango (*Mangifera Indica* L.) Peel Extracts. *ACS Omega* **2021**, *6*, 16119–16128. [CrossRef] [PubMed]
24. Singleton, V.L.; Orthofer, R.; Lamuela-Raventós, R.M. [14] Analysis of total phenols and other oxidation substrates and antioxidants by means of folin-ciocalteu reagent. In *Oxidants and Antioxidants Part A*; Academic Press: Cambridge, MA, USA, 1999; Volume 299, pp. 152–178. ISBN 00766879.
25. Re, R.; Pellegrini, N.; Proteggente, A.; Pannala, A.; Yang, M.; Rice-Evans, C. Antioxidant Activity Applying an Improved Abts Radical Cation Decolorization Assay. *Free Radic. Biol. Med.* **1999**, *26*, 1231–1237. [CrossRef]
26. Kaur, M.; Singh, N.; Sandhu, K.S.; Guraya, H.S. Physicochemical, Morphological, Thermal and Rheological Properties of Starches Separated from Kernels of Some Indian Mango Cultivars (*Mangifera Indica* L.). *Food Chem.* **2004**, *85*, 131–140. [CrossRef]
27. AOAC. *Association of Official Analytical Chemist Official Methods of Analysis*, 17th ed.; AOAC: Gaithersburg, MD, USA, 2000.
28. Morrison, W.R.; Laignelet, B. An Improved Colorimetric Procedure for Determining Apparent and Total Amylose in Cereal and Other Starches. *J. Cereal Sci.* **1983**, *1*, 9–20. [CrossRef]
29. Shi, Z.; Shi, Z.; Wu, M.; Shen, Y.; Li, G.; Ma, T. Fabrication of Emulsion Gel Based on Polymer Sanxan and Its Potential as a Sustained-Release Delivery System for β-Carotene. *Int. J. Biol. Macromol.* **2020**, *164*, 597–605. [CrossRef] [PubMed]
30. Mennen, L.I.; Walker, R.; Bennetau-Pelissero, C.; Scalbert, A. Risks and Safety of Polyphenol Consumption. *Am. J. Clin. Nutr.* **2005**, *81*, 326S–329S. [CrossRef]
31. Williamson, G.; Holst, B. Dietary Reference Intake (DRI) Value for Dietary Polyphenols: Are We Heading in the Right Direction? *Br. J. Nutr.* **2008**, *99*, S55–S58. [CrossRef]
32. Li, L.; Liu, G.; Lin, Y. Physical and Bloom Stability of Low-Saturation Chocolates with Oleogels Based on Different Gelation Mechanisms. *LWT* **2021**, *140*, 110807. [CrossRef]
33. Augusto, P.E.D.; Ibarz, A.; Cristianini, M. Effect of High Pressure Homogenization (HPH) on the Rheological Properties of Tomato Juice: Viscoelastic Properties and the Cox–Merz Rule. *J. Food Eng.* **2013**, *114*, 57–63. [CrossRef]
34. Steffe, J. *Rheological Methods in Food Process Engineering*; Freeman Press: East Lansing, MI, USA, 1996; ISBN 0963203614.
35. Gharibzahedi, S.M.T.; Smith, B.; Guo, Y. Ultrasound-Microwave Assisted Extraction of Pectin from Fig (*Ficus Carica* L.) Skin: Optimization, Characterization and Bioactivity. *Carbohydr. Polym.* **2019**, *222*, 114992. [CrossRef] [PubMed]
36. Pinelo, M.; Sineiro, J. Mass Transfer during Continuous Solid—Liquid Extraction of Antioxidants from Grape Byproducts. *J. Food Eng.* **2006**, *77*, 57–63. [CrossRef]
37. Zou, T.B.; Xia, E.Q.; He, T.P.; Huang, M.Y.; Jia, Q.; Li, H.W. Ultrasound-Assisted Extraction of Mangiferin from Mango (*Mangifera Indica* L.) Leaves Using Response Surface Methodology. *Molecules* **2014**, *19*, 1411–1421. [CrossRef] [PubMed]
38. Dorta, E.; Lobo, M.G.; González, M. Using Drying Treatments to Stabilise Mango Peel and Seed: Effect on Antioxidant Activity. *LWT-Food Sci. Technol.* **2012**, *45*, 261–268. [CrossRef]
39. Guandalini, B.B.V.; Rodrigues, N.P.; Marczak, L.D.F. Sequential Extraction of Phenolics and Pectin from Mango Peel Assisted by Ultrasound. *Food Res. Int.* **2019**, *119*, 455–461. [CrossRef]
40. Adilah, A.N.; Jamilah, B.; Noranizan, M.A.; Hanani, Z.A.N. Utilization of Mango Peel Extracts on the Biodegradable Films for Active Packaging. *Food Packag. Shelf Life* **2018**, *16*, 1–7. [CrossRef]
41. Dorta, E.; González, M.; Lobo, M.G.; Sánchez-Moreno, C.; de Ancos, B. Screening of Phenolic Compounds in By-Product Extracts from Mangoes (*Mangifera Indica* L.) by HPLC-ESI-QTOF-MS and Multivariate Analysis for Use as a Food Ingredient. *Food Res. Int.* **2014**, *57*, 51–60. [CrossRef]
42. Jahurul, M.H.A.; Zaidul, I.S.M.; Ghafoor, K.; Al-Juhaimi, F.Y.; Nyam, K.L.; Norulaini, N.A.N.; Sahena, F.; Mohd Omar, A.K. Mango (*Mangifera Indica* L.) by-Products and Their Valuable Components: A Review. *Food Chem.* **2015**, *183*, 173–180. [CrossRef]
43. Martínez-Ramos, T.; Benedito-Fort, J.; Watson, N.J.; Ruiz-López, I.I.; Che-Galicia, G.; Corona-Jiménez, E. Effect of Solvent Composition and Its Interaction with Ultrasonic Energy on the Ultrasound-Assisted Extraction of Phenolic Compounds from Mango Peels (*Mangifera Indica* L.). *Food Bioprod. Process.* **2020**, *122*, 41–54. [CrossRef]
44. López-Cobo, A.; Verardo, V.; Diaz-de-Cerio, E.; Segura-Carretero, A.; Fernández-Gutiérrez, A.; Gómez-Caravaca, A.M. Use of HPLC- and GC-QTOF to Determine Hydrophilic and Lipophilic Phenols in Mango Fruit (*Mangifera Indica* L.) and Its by-Products. *Food Res. Int.* **2017**, *100*, 423–434. [CrossRef]
45. De Felipe, F.L.; de las Rivas, B.; Muñoz, R. Bioactive Compounds Produced by Gut Microbial Tannase: Implications for Colorectal Cancer Development. *Front. Microbiol.* **2014**, *5*, 684. [CrossRef]
46. Duvivier, P.; Hsieh, P.; Lai, P.; Charle, A. Retention of Phenolics, Carotenoids, and Antioxidant Activity in the Taiwanese Sweet Potato (*Ipomoea Batatas Lam.*) CV Tainong 66 Subjected to Different Drying Conditions. *Afr. J. Food Agric. Nutr. Dev.* **2011**, *10*. [CrossRef]

47. Bharti, I.; Singh, S.; Saxena, D.C. Exploring the Influence of Heat Moisture Treatment on Physicochemical, Pasting, Structural and Morphological Properties of Mango Kernel Starches from Indian Cultivars. *LWT* **2019**, *110*, 197–206. [CrossRef]
48. Patiño-Rodríguez, O.; Agama-Acevedo, E.; Ramos-Lopez, G.; Bello-Pérez, L.A. Unripe Mango Kernel Starch: Partial Characterization. *Food Hydrocoll.* **2020**, *101*, 105512. [CrossRef]
49. Baldwin, P.M. Starch Granule-Associated Proteins and Polypeptides: A Review. *Starch/Staerke* **2001**, *53*, 475–503. [CrossRef]
50. Punia, S.; Kumar, M.; Siroha, A.K.; Kennedy, J.F.; Dhull, S.B.; Whiteside, W.S. Pearl Millet Grain as an Emerging Source of Starch: A Review on Its Structure, Physicochemical Properties, Functionalization, and Industrial Applications. *Carbohydr. Polym.* **2021**, *260*, 117776. [CrossRef] [PubMed]
51. Tagliapietra, B.L.; Felisberto, M.H.F.; Sanches, E.A.; Campelo, P.H.; Clerici, M.T.P.S. Non-Conventional Starch Sources. *Curr. Opin. Food Sci.* **2021**, *39*, 93–102. [CrossRef]
52. Lemos, P.V.F.; Barbosa, L.S.; Ramos, I.G.; Coelho, R.E.; Druzian, J.I. Characterization of Amylose and Amylopectin Fractions Separated from Potato, Banana, Corn, and Cassava Starches. *Int. J. Biol. Macromol.* **2019**, *132*, 32–42. [CrossRef]
53. Tester, R.F.; Karkalas, J.; Qi, X. Starch—Composition, Fine Structure and Architecture. *J. Cereal Sci.* **2004**, *39*, 151–165. [CrossRef]
54. Sandhu, K.S.; Lim, S.T. Structural Characteristics and in Vitro Digestibility of Mango Kernel Starches (*Mangifera Indica* L.). *Food Chem.* **2008**, *107*, 92–97. [CrossRef]
55. Guo, K.; Lin, L.; Fan, X.; Zhang, L.; Wei, C. Comparison of Structural and Functional Properties of Starches from Five Fruit Kernels. *Food Chem.* **2018**, *257*, 75–82. [CrossRef] [PubMed]
56. Hernández-Medina, M.; Torruco-Uco, J.G.; Chel-Guerrero, L.; Betancur-Ancona, D. Caracterización Fisicoquímica de Almidones de Tubérculos Cultivados En Yucatán, México. *Ciência E Tecnol. Aliment.* **2008**, *28*, 718–726. [CrossRef]
57. Tian, S.; Sun, Y. Influencing Factor of Resistant Starch Formation and Application in Cereal Products: A Review. *Int. J. Biol. Macromol.* **2020**, *149*, 424–431. [CrossRef]
58. Samee, M.; Yasin, M.R.; Fatima, S.; Rauf, A.; Naz, S.; Mahpara Gilani, M.T. Comparative Study of Proximate Composition and Mineral Contents in Ctenopharyngoden Idella and Rita Rita Collected from River Chenab. *Int. J. Biosci. IJB* **2018**, *13*, 29–37.
59. Liang, X.; Ma, C.; Yan, X.; Zeng, H.; McClements, D.J.; Liu, X.; Liu, F. Structure, Rheology and Functionality of Whey Protein Emulsion Gels: Effects of Double Cross-Linking with Transglutaminase and Calcium Ions. *Food Hydrocoll.* **2020**, *102*, 105569. [CrossRef]
60. Heydari, A.; Razavi, S.M.A. Evaluating High Pressure-Treated Corn and Waxy Corn Starches as Novel Fat Replacers in Model Low-Fat O/W Emulsions: A Physical and Rheological Study. *Int. J. Biol. Macromol.* **2021**, *184*, 393–404. [CrossRef]
61. Javidi, F.; Razavi, S.M.A.; Mohammad Amini, A. Cornstarch Nanocrystals as a Potential Fat Replacer in Reduced Fat O/W Emulsions: A Rheological and Physical Study. *Food Hydrocoll.* **2019**, *90*, 172–181. [CrossRef]
62. Li, S.; Zhang, B.; Li, C.; Fu, X.; Huang, Q. Pickering Emulsion Gel Stabilized by Octenylsuccinate Quinoa Starch Granule as Lutein Carrier: Role of the Gel Network. *Food Chem.* **2020**, *305*, 125476. [CrossRef]
63. Farjami, T.; Madadlou, A. An Overview on Preparation of Emulsion-Filled Gels and Emulsion Particulate Gels. *Trends Food Sci. Technol.* **2019**, *86*, 85–94. [CrossRef]
64. Kokini, J.; van Aken, G. Discussion Session on Food Emulsions and Foams. *Food Hydrocoll.* **2006**, *20*, 438–445. [CrossRef]
65. Winter, H.H.; Chambon, F. Analysis of Linear Viscoelasticity of a Crosslinking Polymer at the Gel Point. *J. Rheol.* **1986**, *30*, 367–382. [CrossRef]
66. Li, Q.; Xu, M.; Xie, J.; Su, E.; Wan, Z.; Sagis, L.M.C.; Yang, X. Large Amplitude Oscillatory Shear (LAOS) for Nonlinear Rheological Behavior of Heterogeneous Emulsion Gels Made from Natural Supramolecular Gelators. *Food Res. Int.* **2021**, *140*, 110076. [CrossRef]
67. Lu, S.; Yang, Y.; Yao, J.; Shao, Z.; Chen, X. Exploration of the Nature of a Unique Natural Polymer-Based Thermosensitive Hydrogel. *Soft Matter* **2015**, *12*, 492–499. [CrossRef] [PubMed]
68. Xu, Q.; Qi, B.; Han, L.; Wang, D.; Zhang, S.; Jiang, L.; Xie, F.; Li, Y. Study on the Gel Properties, Interactions, and PH Stability of Pea Protein Isolate Emulsion Gels as Influenced by Inulin. *LWT* **2021**, *137*, 110421. [CrossRef]
69. Zhang, Y.; Yang, H.; Zheng, H.; Yuan, D.; Mao, L. Physical Properties and Salt Release of Potato Starch-Based Emulsion Gels with OSA Starch-Stabilized Oil Droplets. *LWT* **2021**, *141*, 110929. [CrossRef]
70. Shahbazi, M.; Jäger, H.; Ettelaie, R. Application of Pickering Emulsions in 3D Printing of Personalized Nutrition. Part I: Development of Reduced-Fat Printable Casein-Based Ink. *Colloids Surf. A Physicochem. Eng. Asp.* **2021**, *622*, 126641. [CrossRef]
71. Rubinstein, M.; Dobrynin, A.V. Associations Leading to Formation of Reversible Networks and Gels. *Curr. Opin. Colloid Interface Sci.* **1999**, *4*, 83–87. [CrossRef]
72. Martins, A.J.; Vicente, A.A.; Cunha, R.L.; Cerqueira, M.A. Edible Oleogels: An Opportunity for Fat Replacement in Foods. *Food Funct.* **2018**, *9*, 758–773. [CrossRef] [PubMed]
73. Chang, Y.Y.; Li, D.; Wang, L.J.; Bi, C.H.; Adhikari, B. Effect of Gums on the Rheological Characteristics and Microstructure of Acid-Induced SPI-Gum Mixed Gels. *Carbohydr. Polym.* **2014**, *108*, 183–191. [CrossRef] [PubMed]
74. Lin, D.; Kelly, A.L.; Miao, S. Preparation, Structure-Property Relationships and Applications of Different Emulsion Gels: Bulk Emulsion Gels, Emulsion Gel Particles, and Fluid Emulsion Gels. *Trends Food Sci. Technol.* **2020**, *102*, 123–137. [CrossRef]
75. Su, D.; Zhu, X.; Adhikari, B.; Li, D.; Wang, L. Effect of High-Pressure Homogenization on the Rheology, Microstructure and Fractal Dimension of Citrus Fiber-Oil Dispersions. *J. Food Eng.* **2020**, *277*, 109899. [CrossRef]

76. Miao, J.; Xu, N.; Cheng, C.; Zou, L.; Chen, J.; Wang, Y.; Liang, R.; McClements, D.J.; Liu, W. Fabrication of Polysaccharide-Based High Internal Phase Emulsion Gels: Enhancement of Curcumin Stability and Bioaccessibility. *Food Hydrocoll.* **2021**, *117*, 106679. [CrossRef]
77. Qi, F.; Wu, J.; Sun, G.; Nan, F.; Ngai, T.; Ma, G. Systematic Studies of Pickering Emulsions Stabilized by Uniform-Sized PLGA Particles: Preparation and Stabilization Mechanism. *J. Mater. Chem. B* **2014**, *2*, 7605–7611. [CrossRef] [PubMed]